FeliX 2.0: An integrated model of climate, economy, environment, and society interactions

Quanliang Ye [a], Qi Liu [b], Deepthi Swamy [c], Lei Gao [d], Enayat A. Moallemi [e], Felicjan Rydzak [f], Sibel Eker [a,c,*]

[a] *Nijmegen School of Management, Radboud University, 6525 XZ, Nijmegen, the Netherlands*
[b] *Business School, Sichuan University, Chengdu, People's Republic of China*
[c] *International Institute for Applied Systems Analysis (IIASA), Laxenburg, 2361, Austria*
[d] *Commonwealth Scientific and Industrial Research Organisation (CSIRO), Waite Campus, Adelaide, SA 5064, Australia*
[e] *Commonwealth Scientific and Industrial Research Organisation (CSIRO), Melbourne, Australia*
[f] *Felix Consultancy, Wroclaw, Poland*

ARTICLE INFO

ABSTRACT

The Full of Economic-Environment Linkages and Integration dX/dt (FeliX) model is a System Dynamics-based Integrated Assessment Model (IAM), explicitly incorporating human behaviors and their dynamic interactions among global systems. This paper presents FeliX 2.0, describing the detailed framework and key interactions among nine integrated modules. FeliX 2.0 refined its original version in population dynamics, food and land use systems, and socioeconomic settings for poverty analysis. Robust calibration is applied to key variables against their historical data since 1950. Future projections of multiple variables up to 2100 demonstrate coherences between FeliX 2.0 and the IAMs used in IPCC assessments. Both outputs (the robust calibration results and future projections) underscore the efficacy of FeliX 2.0 in capturing complex interdependencies within global systems. FeliX 2.0 stands as an informative tool and offers insights into interactions within the human-Earth system and the analysis of complex economic-environmental-social challenges in short- and long-term future.

1. Introduction

Integrated Assessment Models (IAMs) are computational tools designed to simulate linkages in economic-environmental-social systems (Nordhaus, 1993; Schneider, 1997; Schwanitz, 2013; Van Beek et al., 2020). They aim to capture and represent in a simplified way to encompass a multitude of interconnected variables from diverse disciplines, such as greenhouse gas emissions, energy systems, land use, and economic growth. The greatest strength of IAMs lies in their ability to facilitate scenario planning, enabling decision-makers to explore various policy alternatives and understand the trade-offs involved in each option (IPCC, 2022a). By far, IAMs have been widely used for modeling and simulating global challenges such as climate change (IPCC, 2022a; 2022b; Lontzek et al., 2015), sustainable development (Moallemi et al., 2022a; Pedercini et al., 2020), and energy transitions (Pye et al., 2015; Van Vuuren et al., 2016). However, most of existing IAMs tend to overlook feedback perspectives and nonlinear interactions among different real-world systems, potentially introducing inaccuracies into

their predictions (Beck and Krueger, 2016; Schneider, 1997). For example, most IAMs don't endogenize feedback between economy and society or simplify human behavior as stylized demand assumptions driven by externally imposed macro-demographic and socioeconomic trends and/or models (Calvin and Bond-Lamberty, 2018; Van Vuuren et al., 2012). Uncertainties in model inputs and assumptions further complicate their outputs, and the extensive data requirements can be a hurdle in their applications.

A particular way to address IAMs' limitations in recognizing nonlinear interdependencies and feedback within real-world systems is applying System Dynamics (SD) modelling. SD is a well-established methodology with notable applications in understanding and managing systems that change over time (Meadows and Wright, 2008; Sterman, 2000). Widely recognized for its effectiveness, SD has been used in modeling feedback interactions, delayed responses, and non-linear behaviors. Its applications are not only in decision sciences but also within the broader context of the climate and sustainability (Moallemi et al., 2021). Illustrative examples of SD models include the

---

World3 (Meadows et al., 1972), the Integrated Sustainable Development Goals (Millennium Institute, 2021), and the Earth4All (Dixson-Declève et al., 2022). These models simulate how various policies affect human wellbeing, societies, and ecosystems in the short and long term. Two unique features have been recognized, especially for climate- and sustainability-oriented SD models. One is the endogenous modeling of interactions between social, economic, and environmental systems in one integrated model. This feature is in line with the main purpose of IAMs, which seeks to recognize the interlinkages between economic-environmental-social systems. The other feature is the development of representations where relationships between observed outcomes and modeling assumptions are transparent and relatively easy to understand. Aggregate and descriptive SD models can provide valuable complements to insights derived from other Earth system models and detailed IAMs (e.g., partial or general equilibrium) that focus more on a detailed perspective on biophysical and socioeconomic systems but may lack the explicit modelling of feedback between systems.

The Full of Economic-Environment Linkages and Integration dX/dt (FeliX) model is a SD-based IAM that simulates complex interactions among global systems, including population, education, economy, energy, water, land, food, carbon cycle, climate, and biodiversity. The FeliX model is one of the very few models that explicitly incorporate human behavior in the human-Earth systems, considering comprehensive dynamic interactions of socio-economic and environmental sectors. It addresses a key limitation of conventional IAMs (i.e., the limited feedback and nonlinear interactions among systems) and covers the breadth of social, economic, and environmental aspects, and their interactions, in one integrated model. The FeliX model is a continuous model, operating on an annual time scale, and is designed to project global-scale future socioeconomic development and environmental conditions over the long term up to 2100. All the modules in the FeliX model have been calibrated to the historical data. This ensures the reliability of FeliX model in reproducing historical trends and producing plausible projections for the future.

This paper aims to present a systemic and comprehensive framework of the FeliX 2.0 model (shortened to FeliX 2.0 from here on) and describe key interactions among system elements included in FeliX 2.0. The remainder of this paper is organized as follows: Section 2 provides a brief overview of the previous research that used FeliX. Section 3 describes the model by elaborating on variables, functions, and interactions among different modules of FeliX 2.0. Section 3 presents the results about fitness of FeliX 2.0 outputs against historic data, and a comparative analysis of the model's future projections against those of other existing IAMs. Limitations, outlooks, and conclusions of FeliX 2.0 will be summarized in Section 4.

2. Overview of the previous research with the FeliX model

The initial version of FeliX model was presented by Obersteiner et al. (2012) and Rydzak et al. (2013), providing a conceptual description of the dynamic interactions and feedback loops of the model, along with mathematical formulations for all model variables. Based on the FeliX model, researchers have conducted scenario analyses on different global socio-economic and environmental problems. Thereafter, two main research directions, climate change mitigation and sustainable development, have been explored using FeliX.

Climate change mitigation. This direction aims to narrate emission pathways based on different mitigation measures. Walsh et al. (2015) analyzed emission pathways if microalgae was used as a feedstock for livestock and found that up to 2 billion hectares of land currently used for pasture and feed crops could be freed. In a subsequent study, Walsh et al. (2017) projected energy and land-use emissions mitigation pathways through 2100 and found that anthropogenic emissions need to peak before 2025 to maintain realistic pathways to meeting the COP21 emissions and warming targets. Thereafter, the model was extended to FeliX 2.0, focusing on population dynamics, education levels, food and

land use systems including explicit fertilizer use and behavior-driven diet shifts, and socioeconomic settings for global poverty elimination.

Sustainable development. This direction explores how FeliX 2.0 can be employed in assessing the progresses of Sustainable Development Goals (SDGs). Eker et al. (2019) extended the FeliX model by developing a behavioral diet shift module in addition to the food, land use, and agricultural fertilizer consumption modules, and identified the main drivers of global diet change and its implications for the food system. Eker et al. (2019) showed that the social norm effect (for instance, the extent of vegetarianism in the population that accelerates a further switch to a vegetarian diet) and self-efficacy are the main drivers of widespread dietary changes. Moallemi et al. (2022b) implemented the global change scenarios in FeliX 2.0 to explore the impacts of model uncertainty and its structural complexity on the projection of sustainable development under these scenarios. Furthermore, Moallemi et al. (2022a) explored the drivers of progress of global SDGs and found that early planning for systems change into more sustainable pathways was important for accelerating the progress toward increasingly ambitious sustainable targets. Liu et al. (2023) further extended the FeliX 2.0 model with a global poverty module, to assess the effectiveness of different socioeconomic and environmental policies in eliminating poverty and quantified their impacts on the Earth system by 2050. More recently, an indicator for measuring human wellbeing, the global years of good life (YoGL) indicator, was estimated using the FeliX 2.0 model and found to increase by on average about twice the rate by 2100 (Kuhn et al., 2023). The model has been used in further applications to explore sustainable development pathways (Ruan et al., 2023), poverty alleviation strategies (Liu et al., 2023b), and food system transformation (Yang et al., 2023).

3. Structure and module descriptions of FeliX 2.0

The structure of FeliX 2.0 represents relations and interactions between nine real-world global systems: population (including education), economy, energy, water, land, food (including diet change), carbon cycle, climate, and biodiversity. The model outcomes are determined by many interacting feedback loops within and between these systems as shown in Fig. 1 and Table 1.

FeliX 2.0 consists of nice modules, that is, population and education, economy, energy, water, land use and fertilizer use, diet change, carbon cycle, climate, and biodiversity, to stimulate the ten real-world global systems. Key interactions among different modules are listed in Table 1.

3.1. Population and education

In contrast to many IAMs that take population projections as an exogenous input based on different Shared Socioeconomic Pathway (SSP) narratives (Kc et al., 2018; Riahi et al., 2017), the population module is endogenous and conceptualized based on dynamic mechanisms of population development and population ageing. Population development is governed by the population growth mechanism and the balancing effect of economic growth and education. The growth mechanism captures how a growing population leads to a higher economic output and how the economic growth increases the life expectancy at birth, reduces mortality, and hence further increases the population. The balancing effect mainly describes effects of increasing economic outputs and educational attainment decreasing fertility rates. The interaction of the feedback mechanism allows for simulation of population ageing.

3.1.1. Ageing structure

Population growth is based on an ageing chain and computes the male and female population size of 5-year age groups between 0 and 100+ years old (Fig. 2). The ageing chain represents the transition of newborns through the age cohorts as they age. It means that each age cohort (except the "0–4" cohort) has one inflow (maturation of the previous cohort) and two outflows (maturation to the next cohort and
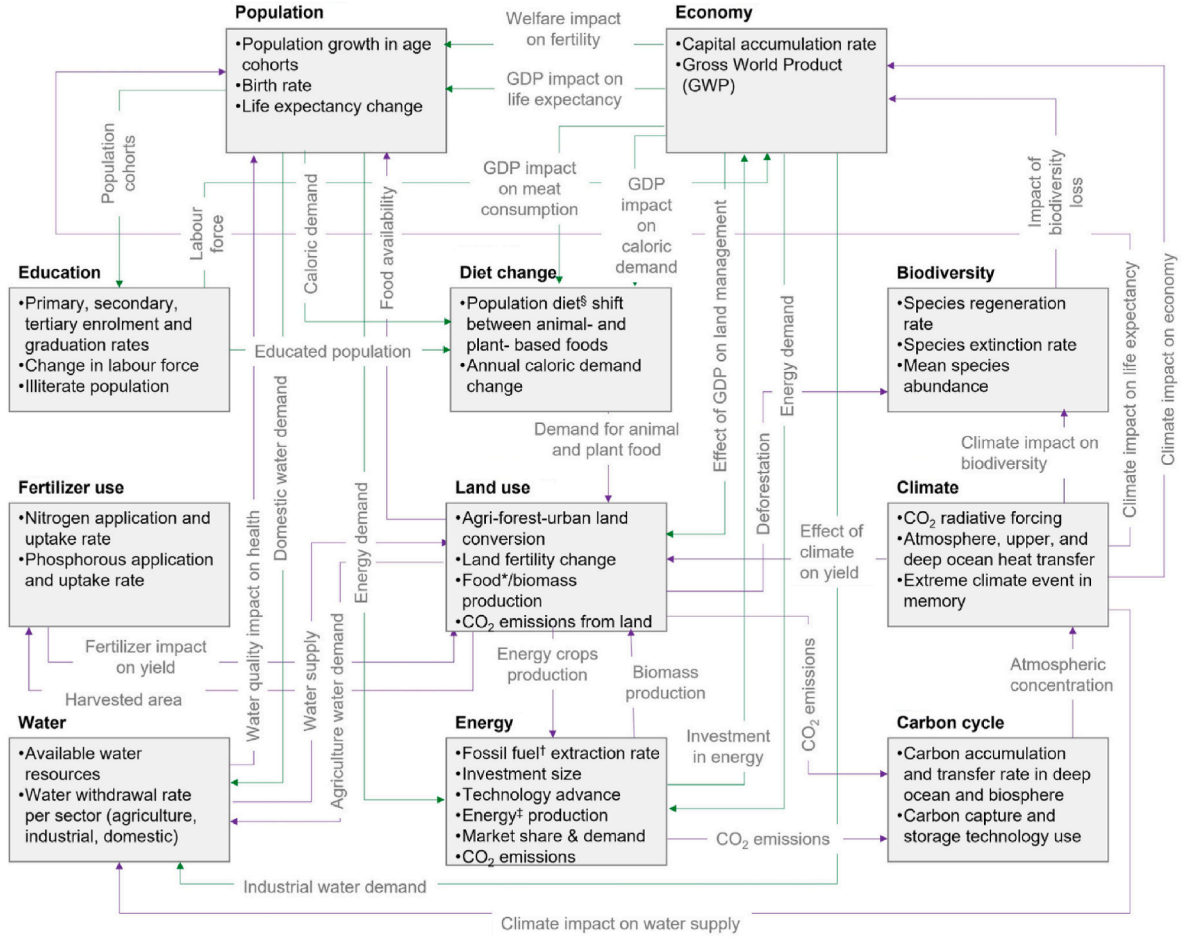
Fig. 1. Overview of FeliX 2.0. We include 11 components in the figure to better illustrate interactions within and among the modules. As such, education shows as a separate component from population, and fertilizer use shows separate from land use. Source: Moallemi et al. (2022).

mortality). Population of each gender and age interval ($Pop_{gender,age}$, Eq. (1)) accumulates by three flows, determining the net rate of change ($dPop/dt$). These three flows are birth rate ($Birth_{gender,age}$), death rate ($Death_{gender,age}$), and maturation rate ($Matur_{gender,age}$) by gender and age.

$$\frac{dPop_{gender,age}}{dt} = \begin{cases} Birth_{gender}(t) - Matur_{gender,age}(t) - Death_{gender,age}(t); \; if \; age = "0-4" \\ Matur_{gender,age-1}(t) - Matur_{gender,age}(t) - Death_{gender,age}(t); \; if \; "5-9" < age < "95-99" \\ Matur_{gender,age-1}(t) - Death_{gender,age}(t); \; if \; age = "100+" \end{cases} \qquad (1)$$

$Matur_{gender,age}$ is formulated as the division of population by the interval duration ($Intvl\_Dur$, 5 years). It assumes a homogenous distribution of population within the age group.

3.1.2. Birth rate and fertility

The birth rate ($Birth_{gender}$, Eq. (2)) is the main factor affecting population dynamics, alongside the reproductive female population represented by gender and age-cohort segmentation. The birth rate is driven by education, and wealth represented by gross world product (GWP) per capita (GWP_per_Cap).

$$Birth_{gender}(t) = g_{gender} \times \frac{\sum_{age="15-19"}^{"45-49"} Pop_{female,age}(t) \times Fert_{age}(t)}{Intvl\_Dur} \qquad (2)$$

where g_{gender} denotes the birth gender fraction, i.e., gender fraction of

registered newborns. $Fert_{age}$ refers to the age-specific fertility rate, which is the number of births per woman in a particular age group during a 5-year period. $Fert_{age}$ is formulated as a function of total fertility (Tot_Fert).

$$Fert_{age}(t) = L0_{age} + \frac{L_{age}}{1 + e^{-k_{age} \times (Tot\_Fert(t) - x0_{age})}} \qquad (3)$$

Eq. (3) is formulated as a logistic function, with parameters, $L0_{age}$, L_{age}, k_{age}, and $x0_{age}$, calibrated based on historical data obtained from the Wittgenstein Centre Human Capital Data Explorer (Wittgenstein Centre, 2020). This formula of logistic functions is extensively used in FeliX 2.0 to estimate impacts of a certain factor on interested variables. In consideration of the space limit in the main text, we refrain from providing a detailed elaboration of each logistic function from here on. Details about the logistic functions are available in the supplementary model documentation (Ye and Eker, 2024).

Tot_Fert represents the number of births per woman at reproductive

Table 1
Main interactions within and among modules in FeliX 2.0. The interactions are direct interactions, always from the row modules to the column modules.

From	To								
	Population and education	Economy	Energy	Water	Land use and fertilizer use	Diet change (food demand)	Carbon cycle	Climate	Biodiversity
Population and education	• Demographic dynamics • Population cohorts to graduates from different educational levels	• Population and education levels determining skill-differentiated labor force as a driver of economic output. • Population and education levels determining poverty rate	• Total population to estimate total energy demand	• Total population to estimate total water demand		• Age and gender-differentiated population to estimate total caloric demand • Age, gender and education levels influencing diet shifts			
Economy	• Wealth influencing fertility, life expectancy and education enrollment rates		• Wealth influencing per-capita energy demand	• Economic development influencing industrial water demand	• Economic development influencing land management, agricultural management practices and fertilizer consumption	• Wealth influencing per-capita caloric demand • Wealth influencing per-capita meat consumption			
Energy		• Investment in energy technologies driving the capital and technology components of economic output	• Energy production requiring investment in energy technology • Market competition among energy technologies		• Biomass-based energy demand determining biomass production and land use change		• Energy production contributing CO_2 emissions		
Water	• Water quality impacting human health				• Water supply influencing crop yields				
Land use, fertilizer use and food production	• Food availability impacting population via life expectancy		• Land availability affecting biomass-based energy production	• Agricultural production determining agricultural water demand	• Land pressure influencing fertilizer demand • Fertilizer use influencing crop yields	• Food supply and health impacts affecting diet change	• Land use change contributing CO_2 emissions		• Land use change impacting biodiversity • Biomass production (both forest and crop) impacting biodiversity • N and P leaching from fertilizer use impacting biodiversity
Diet change					• Food demand determining production of animal and plant foods				
Carbon cycle								• CO_2 emissions contributing	

Table 1 (*continued*)

Climate	• Climate impacting life expectancy	• Climate impacting economic output	• Climate impacting water supply	• Climate impacting crop yields	• Climate risk perception impacting behavior change	• Temperature change affecting carbon flux between atmosphere and ocean (cooling feedback)	atmospheric concentration	• Climate impacting biodiversity
Biodiversity	• Biodiversity loss impacting economic output							

ages (between 15 and 50). It considers the effects of education (*Imp_Edu_on_Fert*) and wealth on fertility (*Imp_GWP_on_Fert*).

$$Tot\_Fert(t) = Norm\_Fert \times Imp\_Edu\_on\_Fert(t) \times Imp\_GWP\_on\_Fert(t) \tag{4}$$

where *Norm_Fert* is the reference value of fertility, equal to the historical value of 2.63 births per woman in year 2000. This formulation also prevents a strong assumption on the monotonic dependence of fertility solely on education or solely on economic output. *Imp_Edu_on_Fert* and *Imp_GWP_on_Fert* are formulated as logistic functions based on mean years of schooling and *GWP_per_Cap*, respectively.

3.1.3. Mortality rate and life expectancy at birth

Death rate ($Death_{gender,age}$) refers to the number of people who pass away in each gender and age group per year. It is formulated as a fraction of the population of each group.

$$Death_{gender,age}(t) = Pop_{gender,age}(t) \times Mort_{gender,age}(t) \tag{5}$$

where $Mort_{gender,age}$ is the mortality fraction by gender and age cohort. $Mort_{gender,age}$ is calculated as a logistic function of global average life expectancy at birth (*LE*). *LE* is derived through a multiplicative function considering impacts of wealth, education, total food supply, and climate change on a reference value of *LE*–the observed life expectancy at birth in 2000. The impacts on life expectancy stemming from wealth, education, and total food supply are estimated by logistic functions based on *GWP_per_Cap* (The World Bank, 2020), mean years of schooling (Wittgenstein Centre, 2020), and total daily calorie supply per capita (FAOSTAT, 2020a), respectively. The last impact, climate change's effect on *LE* (*Imp_CC_on_LE*), is estimated depending on future temperatures. Global temperature rise is the main driver of climate mortality–the death rate directly attributed to the impacts of climate change such as extreme weather events, rising temperatures, and related environmental changes (IPCC 2022b). Meanwhile, education is expected to mediate climate mortality. To quantify *Imp_CC_on_LE*, climate change impacts on mortality (*Imp_CC_on_Mort*) is estimated firstly, by taking into account both temperature and education and calibrated to the estimates of Bressler et al. (2021). *Imp_CC_on_LE* is inversely proportional to *Imp_CC_on_Mort*.

$$Imp\_CC\_on\_LE = \frac{1}{1 + IMP\_CC\_on\_Mort(t)} \tag{6}$$

Finally, *LE* is converted to life expectancy for each gender and age group ($LE_{gender,age}$) with constant coefficients, which are estimated as the mean of historical values between 1990 and 2020. Associated data is obtained from the Global Burden of Disease dataset (Lopez and Murray, 1998).

3.1.4. Educational attainment and mean years of schooling

3.1.4.1. Educational attainment. Population by age cohort serves as input into the education module to compute the population of primary, secondary, and tertiary education graduates according to the enrollment rates and graduation rates (Fig. 1). Population with each educational attainment level, similar to the population chain, accounts for the ageing of people who graduate from each level and for transitions between the education levels. In detail, primary, secondary, and tertiary education graduates accumulate by each gender and 5-year age group corresponding to the respective education level. The assumptions regarding the age groups corresponding to education levels are as follows: children aged 5–9 enroll in primary education, with an average duration of 6 years. Subsequently, primary graduates, aged 10–14 or 15–19, may proceed to secondary education for another 6 years. Tertiary education enrollment is limited to the "15–19", "20–24", and "25–29" age groups, with an average duration of 5 years.
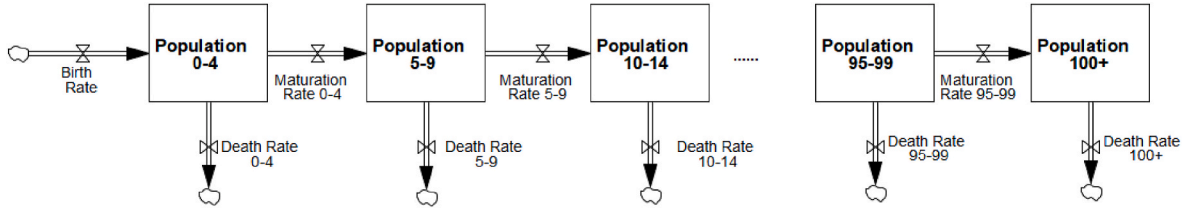
Fig. 2. Inflows and outflows to different population cohorts in the population module. Population cohorts also distinguish gender into male and female. According to the System Dynamics methodology, boxes represent stocks/accumulations of elements while the arrows represent in-flows and out-flows indicating the direction of movement of quantities between stocks.

Net change rate of primary education graduates ($dPEG/dt$) for each gender-age group is formulated as:

$$\frac{dPEG_{gender,age}(t)}{dt} = \begin{cases} 0; \text{ if age in } \{"0-4", "5-9"\} \\ Grad\_Prim_{gender,age}(t) - Enrl\_Sec_{gender,age}(t) - Matur\_Prim_{gender,age}(t) - Death\_Prim_{gender,age}(t); \text{ if age in } \{"10-14", "15-19"\} \\ Matur\_Prim_{gender,age-1}(t) - Matur\_Prim_{gender,age}(t) - Death\_Prim_{gender,age}(t); \text{ if age } > "20-24" \end{cases} \quad (7)$$

where $Grad\_Prim_{gender,age}$ is graduation rate from primary education, which is equal to enrollment rate to primary education ($Enrl\_Prim_{gender}$) yet after a delay of average duration of primary education. $Enrl\_Prim_{gender}$ is calculated by multiplying the population at the age of 5–9 with the primary education enrollment fraction for each gender (PEF_{gender}). PEF_{gender} is defined as a reference value (Ref_PEF_{gender}, as the maximum possible enrollment fraction) multiplied by the impact of wealth ($Imp\_GWP\_on\_Prim_{gender}$). $Imp\_GWP\_on\_Prim_{gender}$ is formulated as a logistic function and calibrated based on GWP_per_Cap.

$$PEF_{gender}(t) = Ref\_PEF_{gender} \times Imp\_GWP\_on\_Prim_{gender}(t) \quad (8)$$

$Matur\_Prim_{gender,age}$ and $Death\_Prim_{gender,age}$ in Eq. (7) are maturation and death rates of primary education graduates, respectively, which is proportionally to the ratio between $PEG_{gender,age}$ and $Pop_{gender,age}$.

The formulation of secondary and tertiary education graduates follows Eqs. (7) and (8), with differences in the age groups explained in the list of assumptions above. Enrollment to secondary (tertiary) education is assumed to be fraction of the primary (secondary) education graduates, implying that the previous education level is a prerequisite for enrollment. The effect of GWP on enrollment for each education level is calibrated to historical data from WCDE for the period 1950–2020 (Wittgenstein Centre, 2020).

3.1.4.2. Mean years of schooling (MYS).
Mean years of schooling serves as a crucial metric in delineating the effect of education on fertility rates and life expectancy. Mean years of schooling is formulated as the weighted average of the duration of each education level. The weights are determined by the total number of graduates for the respective education level relative to the population aged 15 and above.

3.1.5. Labor force
Labor force is distinguished as skilled ($LF_{skilled}$) and unskilled labor force ($LF_{unskilled}$). The skilled labor force is the sum of total population aged 15–64 with tertiary education and half of the population aged 15–64 with secondary education. The unskilled labor force is determined by the remaining population aged 15–64.

3.2. Economy

The economy module is based on the Cobb-Douglas production function, where Gross World Product (GWP), that is, global total GDP, is computed from labor input, total capital input from the energy and non-

energy sectors, and total factor productivity from energy and non-energy technologies. The Cobb-Douglas function is also incorporated the impacts of changes in ecosystems and climate change on the economic outputs. The assessment of global poverty rate is also included in the economy module.

3.2.1. Gross world product (GWP)
GWP is determined by the total reference economic output (REO). The total REO is the sum of the REO generated by the labor force by skill (REO_{skill}). Skilled and unskilled labor force are distinguished. REO_{skill} are computed based on a Cobb-Douglas production function, depending on the technology (φ_Tech_{skill}) and capital (φ_K_{skill}) allocated to the labor force, and the size of the labor force.

$$REO_{skill}(t) = REO\_Init_{1900,skill} \times \varphi\_Tech_{skill}(t) \times Tech(t)$$
$$\times \left(\varphi\_k_{skill}(t) \times \frac{K(t)}{K_{Init}} \right)^{CEO_{skill}}$$
$$\times \sum_{gender} \sum_{age="15-19"}^{"60-64"} LF_{gender,age,skill}(t)^{(1-CEO_{skill})} \quad (9)$$

where CEO_{skill} is the capital elasticity output for skilled and unskilled labor force. $REO\_Init_{1900,skill}$, φ_Tech_{skill}, φ_K_{skill}, and CEO_{skill} are exogenous parameters determined by model calibration based on historical data of GWP and GWP_per_Cap from The World Bank (2020). K and K_Init are annual capital stock and initial capital stock in 1900, respectively. Technology-related factor productivity ($Tech$) is distinguished into energy technology ($Tech\_Eng$) and all other technology ($Tech\_Oth$). Particularly, $Tech\_Eng$ is endogenously determined by investments in the energy module while $Tech\_Oth$ follows an exogenous trend and data. The labor force ($LF_{gender,age,skill}$) is the corresponding labor force by different skills multiplied by the labor force participation rates for the respective groups (by gender and age cohort), which is set to be 34–78% depending on genders and age cohorts following The World Bank (2020).

3.2.2. Climate change impacts on GWP
Impacts of climate change on economy ($Imp\_CC\_on\_GWP$) assumes that the temperature change has a direct impact on the economic output, following the commonly used 'damage function' forms presented by Nordhaus (2017), Dietz and Stern (2015), Burke et al. (2015), and a custom function defined in a flexible logistic form. The baseline damage assumption follows the estimates of Burke et al. (2015) which reach almost 75% of GDP loss at 5 °C of warming for the case where long-run (5 year) effects of temperature change are considered and countries give differentiated adaptation response. Details about the damage functions
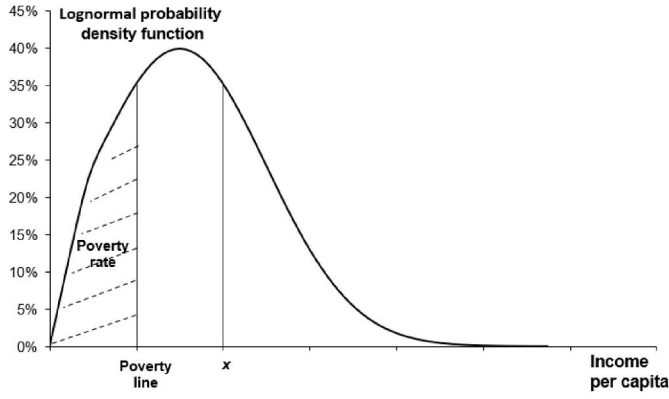
Fig. 3. The lognormal probability density function of income. The shaded area is equal to the poverty rate.

(DFs) are available in (Eker et al., 2023) and Ye and Eker (2024).

3.2.3. Poverty

The global poverty rate (*PR*) is defined as the proportion of the population aged 15+ living below the international extreme poverty line (*PL*). The global *PR* is calculated as the sum of the poverty rates across the different population groups aged over 15 ($PR_{gender,age}$) weighted by their corresponding population shares. In addition, *PL* is defined as minimum consumption or income of a person per day and set as \$2.15 per capita per day in 2017 PPP by The World Bank (2022). Income per capita by gender and age cohort ($Income\_per\_Cap_{gender,age}$) is used to calculate $PR_{gender,age}$ (Fig. 3, Fosu, 2010; Hughes, 2015). $Income\_per\_Cap_{gender,age}$ is assumed to follow a log-normal distribution characterized by the mean $\mu_{gender,age}$ and standard deviation $\sigma_{gender,age}$ of the normal distribution function of $\ln\left(Income\_per\_Cap_{gender,age}\right)$, based on previous research (Fosu, 2010; Lakner et al., 2022; Liu et al., 2023a).

$$PR_{gender,age}(t)\left(Income\_per\_Cap_{gender,age} \leq PL\right) = \varnothing\left(\frac{\ln(PL) - \mu_{gender,age}(t)}{\sigma_{gender,age}(t)}\right) \tag{10}$$

The value of a standard normal cumulative distribution function can be obtained by looking up the standard normal distribution table. $Income\_per\_Cap_{gender,age}$ is related to the GWP per capita.

$$Income\_per\_Cap_{gender,age}(t) = GWP\_per\_Cap(t) \times Real\_Income\_Param_{gender,age} \tag{11}$$

where $Real\_Income\_Param_{gender,age}$ is determined by model calibration according to the data from The World Bank (2020).

3.3. Energy

The energy module includes total energy demand and energy supply from different fossil fuels (oil, gas, coal) and renewable energy (wind, solar, biomass).

3.3.1. Energy demand

Global energy demand is determined by the per-capita energy demand and the global population. The energy demand per capita (*En_Dem_per_Cap*) is determined by the wealth of the population.

$$En\_Dem\_per\_Cap(t) = Imp\_GWP\_on\_En\_Dem(t) \times En\_Dem\_per\_Cap\_Max \tag{12}$$

Imp_GWP_on_En_Dem represents the impact of *GWP* on *En_Dem_per_Cap*. It is modeled as a non-linear relationship—initially increasing at a low rate, then at an increased rate and eventually flattens out over the long run. Furthermore, *Imp_GWP_on_En_Dem* is calibrated

according to the historical energy demand pattern obtained from Energy Institute (2023). *En_Dem_per_Cap_Max* is the maximal reference of energy demand per capita.

3.3.2. Energy production

Energy production comes from three fossil fuels (coal, oil, and gas) and three renewable (solar, wind, and biomass) sources, to meet the total energy demand. The production of any type of energy is determined by its identified resource and production capacity, and its market share.

3.3.2.1. Energy production from fossil fuels.
The production of fossil fuels is modeled as a supply chain structure, adapted from Sterman and Richardson (1985) and Davidsen et al. (1990). This section uses oil as an example to explain main components of the energy production structure for fossil fuels. In general, oil is produced from identified oil resources, which grows based on oil exploration through existing technologies from undiscovered oil resources.

Oil exploration ($Expl_{oil}$) is counted as the lower value of a potential exploration rate of oil ($Expl\_Pot_{oil}$) and a desired exploration rate of oil ($Expl\_Des_{oil}$). $Expl\_Pot_{oil}$ represents the exploration possible due to effective investments in oil exploration ($Eff\_Expl\_Inv_{oil}$) and productivity of available technologies ($Prodvty\_Expl\_Inv_{oil}$) which encapsulates the resource depletion effect.

$$Expl\_Pot_{oil}(t) = Eff\_Expl\_Inv_{oil}(t) \times Prodvty\_Expl\_Inv_{oil}(t) \tag{13}$$

$Expl\_Des_{oil}$ represents the amount of oil resources that would ensure continued production at the current rate. Unit cost of oil exploration is then estimated depending on the remaining undiscovered oil resources and advances in exploration technologies. The cost of oil exploration in turn determines the desired investment in oil exploration.

Similarly, the oil production is counted as the lower value of either total oil demand or a potential oil production rate. The total oil demand is calculated as the market share of oil in total energy demand. The potential oil production rate equals to the production due to effective investments in oil production and available resources. Similar to the costs of exploration, the unit cost of oil production is then dependent on the productivity of investment in oil production which encapsulates the resource availability effect. It is important to note that production costs also include the policy-set carbon price. The cost of both oil exploration and production determines the oil price, which affects the market share of oil demand in total energy demand (see section **2.3.3 Market shares of energy sources in total energy demand**).

3.3.2.2. Energy production from renewable sources.
There are several main factors that affect the production of renewable energy from wind, solar, and biomass sources. They are resource characteristics (e.g., average sun radiation for solar energy), efficiency and aging of technology, land availability, installation cost, investment in installation and efficiency, and the impact of technological learning on unit costs of installation. This section uses solar energy as an example to explain important dynamics in the structure underlying renewable energy production.

Firstly, total solar demand equals to the market share of solar energy multiplied by the total energy demand. Secondly, the solar production capacity is calculated to meet total solar demand but constrained by the potential solar energy production. The potential solar energy production depends on the available solar resource and technological constraints of average intensity of the resource, annual availability of the resource considering weather impacts, changing efficiency of solar radiation conversion at the current state of technical developments, and the installed capacity to convert solar radiation into energy. The installed solar capacity changes according to the new installation of solar capacity, which is influenced by the productivity of solar investments and the adjustment of existing solar infrastructure. Lastly, the unit cost of

solar energy is estimated as a sum of the unit costs of installation and production.

3.3.3. Market shares of energy sources in total energy demand

The total energy demand is allocated to different energy sources based on their respective market shares (*MS*). *MS* is calculated based on indicative market shares (*MS_Ind*) of energy sources which are defined to represent accumulated market shares of different energy sources over time.

$$MS_{energy}(t) = \frac{MS\_Ind_{energy}(t)}{\sum\limits_{energy} MS\_Ind_{energy}(t)} \qquad (14)$$

MS_Ind of a specific energy is determined by effects of price on the market share (*Eff_MS_Price*) and time to adjust the market share (*Time_Adj*).

$$\frac{dMS\_Ind_{energy}(t)}{dt} = \frac{MS\_Ref_{energy} \times Eff\_MS\_Price_{energy}(t) - MS\_Ind_{energy}(t)}{Time\_Adj}$$

where *MS_Ref_energy* is the reference market share of a specific energy source. *Time_Adj* is set as 10 years for all energy sources. *Eff_MS_Price* depends on the competitive price factors and prices of energy sources. The price of each energy source is averaged over a period, and all the prices result in the average energy price. The price competitive factor is calculated for all energy sources as a ratio of the averaged price of each energy source and the average energy price. The price competitive factor is further adjusted by the elasticity of that energy source price to demand.

3.4. Water

The water module mainly quantifies global average water scarcity, that is, the balance between water availability and use. Water availability is a function of available water resources, water recovery of used water in economic sectors, and a drought rate for the impact of climate change. Total water use considers water withdrawal by three economic sectors (agriculture, industry, and domestic) to meet their water demands.

3.4.1. Water supply and water availability

Available water resources consist of water supply rate of fresh and non-conventional water, water recovery rate of used water resources by the three economic sectors, and drought out rate representing extreme drought events. Water supply is estimated by multiplying desired water supply rate and water supply fulfillment rate (describing water supply fulfillment as a relation of water supply and demand). Desired water supply rate $\left(Wat\_Sup\_Des\right)$ is to cover water consumption (*Wat_Cons*, i.e., water use decreased by recovery of used water resources of three economic sectors) and available water resources adjustment (*Wat_Avail_Adj*, taking into account dynamics of total water demand and water safety stock coverage).

$$Wat\_Sup\_Des(t) = MAX(0, Wat\_Cons(t)) + Wat\_Avail\_Adj(t) \qquad (15)$$

With growing water demand, the supply fulfillment might be impaired which relates to infrastructure design and its operating limits. This relationship is modeled as a logistic function dependent on the amount of water that can be reliably provided on annual basis for agricultural, industrial, and domestic sectors due to resources and infrastructure availability. Associated data are obtained from 2030 Water Resources Group (2009).

3.4.2. Water demand, water withdrawal, and water use

Water is demanded for economic production by agriculture, industrial, and domestic sectors. Agricultural water demand (*Wat_Dem_Agri*) is dependent on two ways of land watering–irrigation and rainfed.

$$Wat\_Dem\_Agri(t) = Wat\_Int\_Irr(t) \times Area\_Irr(t) + Wat\_Int\_Rfed(t)$$
$$\times Area\_Rfed(t)$$
$$(16)$$

where *Wat_Int_Irr* and *Wat_Int_Rfed* represent average agricultural water demand per square (i.e., water intensity, *Wat_Int*) agricultural land areas of irrigation (*Area_Irr*) or rainfed (*Area_Rfed*), respectively. *Area_Irr* is calculated by multiplying total agricultural land areas with the percentage of irrigated land areas, which is estimated by considering the impact of wealth (represented by *GWP_per_Cap*) and their upper and lower limits. This approach is also applied to estimate *Wat_Int_Irr*, *Wat_Int_Rfed*, and total water demand for industrial sector based on their own upper and lower limits, respectively. Domestic water demand is quantified based on total population and average domestic water demand per capita. Domestic water demand per capita is estimated by considering the impact of wealth (represented by *GWP_per_Cap*) and their upper and lower limits.

Agricultural, industrial, and domestic water demand drives water resources withdrawal from available water resources. Similar to water supply, agricultural, industrial, and domestic water withdrawal rates slow down when their demands approaching max water withdrawal rate. This process is represented by water withdrawal fulfillment rate (*Fulf_Rat_Withd*). Particularly for agricultural water withdrawal (*Wat_Withd_Agri*), impacts from extreme drought (*Drght_Rat*) is also considered to simulate the decrease in *Wat_Withd_Agri* and available water resources due to drought.

$$Wat\_Withd\_Agri(t) = Wat\_Dem\_Agri(t) \times Fulf\_Rat\_Withd(t) \times (1 - Drght\_Rat)$$
$$(17)$$

Agriculture, industrial, and domestic water withdrawal rates accumulate as total used water resources. As mentioned in the section **Water supply and water availability**, a fraction of total used water resources can be recovered and supplied as available water resources.

3.5. Land use and fertilizer use

The global land use and land use change dynamics are represented based on four main categories of land use as defined by FAO (FAOSTAT, 2020a): agricultural, forest, urban/industrial, and the other land that does not fall into any of the first three categories. Land use change refers to the conversion of land among these four categories. Considering the historical and expected dynamics, a bi-directional conversion between the agricultural land and forest land and between the agricultural land and other land is assumed. The rest of land use changes are considered one directional conversion, that is, from agricultural land to urban and industrial land, from forest land to urban and industrial land, and from other land to forest land (Fig. 4).
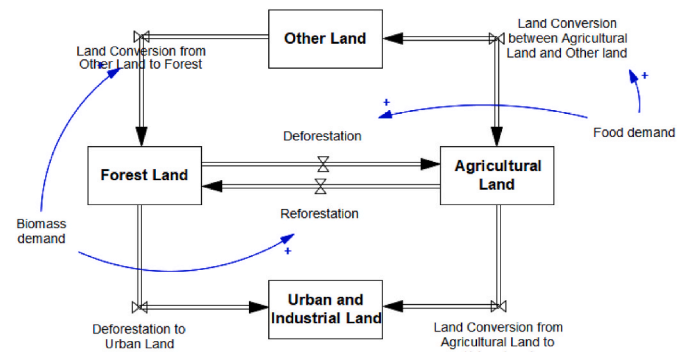

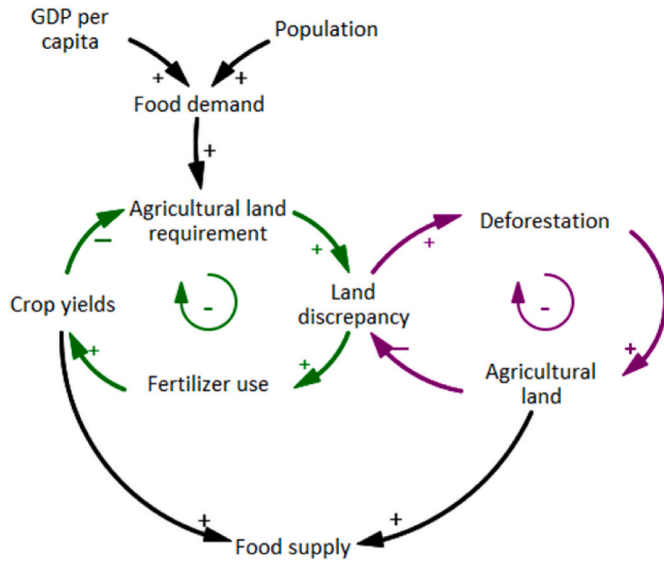**Fig. 4.** Stylized stock-flow diagram of the land use module.

Fig. 5. Stylized feedback loops driving the land use change in FeliX.

3.5.1. Land conversion

The main underlying driver of land use change is the food system, in addition to bioenergy and forest management practices (Fig. 4). Each land category is modeled as a stock. Apart from urban and industrial land, which is set to increase only, all other types of land can gain more space or lose it due to land conversion. For instance, abandoning any human activities in a part of agriculture land and allowing certain duration of time the agriculture land will be covered by grass, later by shrubs, yet later by trees and eventually it will be classified as forest. The easier it is for the natural process to transform the area the transformation time is set to a lower value. In case of forest–agriculture land conversion, agriculture–other land conversion, and other–forest land conversion, there are additional forces apart from natural conversion processes that drive and increase the rate of expansion or shrinking of the forest, other and agriculture land areas. A constant ratio is set for other land and forest land areas as protected land, respectively. In case of forest land, the protected area increases successively. The protected areas are excluded from any transformation processes. The agricultural land requirements and its estimates will be especially elaborated in the next section due to the key link with diet change module (Fig. 1).

3.5.2. Agricultural land requirements

Agricultural land requirement increases due to the growing population and income levels which lead to more food demand (Fig. 5). Agricultural land is further divided into three sub-categories as arable land, permanent cropland, and permanent meadows and pastures. Land use shifts due to food demand are considered based on plant- and animal-based food that have their own land allocation and yields. Eight categories of food products are specified and sorted into plant-based and animal-based food. Plant-based food include pulses, grains, vegetables and fruits, and other crops such as sugar and oil crops. Animal-based food are pasture-based meat, crop-based meat, dairy, and eggs. This categorization of especially animal products were motivated by the land use shares: The pasture-based meat category includes the red meat sources such as beef, sheep and goat, since 96% of the global average land use per unit of beef production is attributed to pasture land, that is, 12 of 12.5 ha per million kcal (Ranganathan et al., 2016). As for poultry and pork, the average land use footprint is less than 2 ha, while a large portion of this is on cropland (Ranganathan et al., 2016), since grains provide the 71% of the total feed demand (FAOSTAT, 2020a).

For each plant-based food, the arable land needed (ALN) is formulated according to the desired production rate (Prod_Des) and the expected crop yield (Yield_Exp), which is a 1-year time-averaged value of the crop yield over time.

$$ALN_{food}(t) = \frac{Prod\_Des_{food}(t)}{Yield\_Exp_{food}(t)},$$

(18)

where $food \in [pulses, grains, vegetables\ and\ fruits, other\ crops]$

Prod_Des$_{food}$ of each plant crop is the sum of the demand for that crop to be used as food, livestock feed, and in other sectors. The estimate procedures of crops to be used as food and livestock feed are described in section **2.6 Diet Change**. Crop to be used in other sectors is quantified as a constant ratio of total plant-based food demand. The actual production of each plant crop is the lower value of Prod_Des$_{food}$ and the production volume calculated as crop yield multiplied by the area harvested. Crop yield is formulated with respect to a reference yield values in 2016 with the dynamic multiplicative impact of fertilizer application, water withdrawal rate and technology change. The total agricultural land requirements are estimated by dividing ALN$_{food}$ by the annual share of arable land in the total agricultural land. The rest of agricultural land is proportionally distributed as permanent cropland and permanent meadows and pastures according to their annual share in agricultural land.

The discrepancy between agricultural land requirement and available agricultural land pushes agricultural production systems either towards more fertilizer use to increase the crop yields and reduce the land requirement, or to deforestation and other land requisition to expand the agricultural land. Eventually, food supply is dependent on the land available, hence harvested, for each food category, and the crop (or meat) yields that depend on fertilizer use, water availability and other agricultural management practices.

3.5.3. Fertilizer use

Nitrogen and phosphorus fertilizer use in agriculture, from commercial sources or livestock manure, is explicitly modeled. Both nitrogen and phosphorus use, as well as their impacts, are modeled in a similar framework that focuses on chemical inflows to and outflows from agricultural land. This section uses phosphorus (P) as an example to explain the framework.

Global P balance with major inflows and outflows (Fig. 6) is based on an input and output framework (MacDonald et al., 2011) and a former modeling study about the biochemical processes of phosphorus (Dumas et al., 2011). In general, the global P residual in soil grows due to the application of commercial P fertilizers and the application of manure as a fertilizer, and decreases due to the uptake by crops and the loss of P via erosion, leaching to freshwater systems and surface runoff. The residual P and flows are reported in terms of the volume of elemental P, except the commercial fertilizer production and application, which are
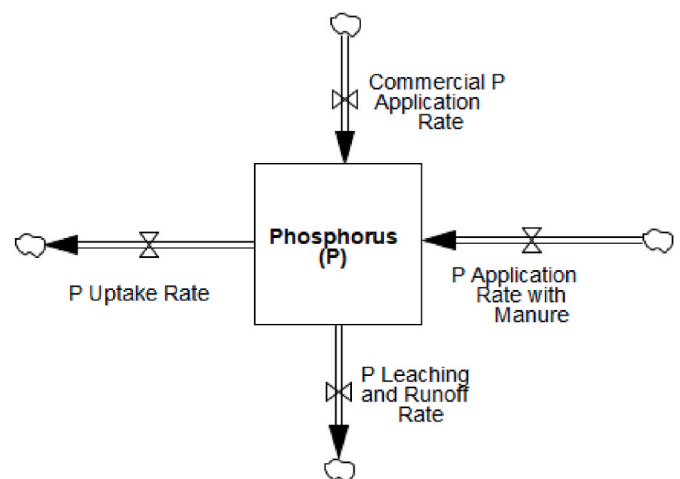

Fig. 6. Agricultural phosphorus inflows and outflows.

reported as the volume of P_2O_5 content. The application of commercial P fertilizers is modeled as the minimum of P demand from agriculture and P supply for agriculture. P demand from agriculture is formulated based on a reference application rate, taking into account the effect of income levels and land scarcity. Both effects are formulated as logistic functions based on *GWP* and the ratio between global agricultural land demand and the available agricultural land, respectively. Supply for agriculture is a fraction of the total P via P rock extraction. This fraction is set as 0.9, since the agricultural use has been on average 90% of the total P_2O_5 produced between 2002 and 2015 (FAO, 2018). P uptake by crops are estimated as a weighted average of the P contents in individual food category, using the data from USDA Food Composition Databases (USDA, 2020). We assume a nonlinear relation between P uptake and crop yields, based on the agronomic nonlinear dynamics of crop growth (Yin and Struik, 2010) that result in sigmoid growth.

3.6. Diet change

Food demand is quantified based on the total caloric demand for eight main food categories. Total caloric demand is based on dietary choices of different population segments. Population segments of dietary choices are represented by the followers of the meat-based and vegetarian diets for each age cohort and gender (Eker et al., 2019). The shifts between these two dietary choices depend on income (represented by *GWP_per_Cap*) and social and behavioral factors such as climate and health risk perception, self-efficacy and social norms that underly pro-environmental behavior.

Followers of meat-based and vegetarian diets are assumed to eat a standard mix of eight food categories. Typical United States' diets (Pimentel and Pimentel, 2003), a reference world diet and the global average supply statistics, were used as benchmarks to understand how meat-based and vegetarian diets differ globally. Based on such proportional differences of meat-based and vegetarian diets, the reference meat-based and vegetarian diets were formed by decomposing the world's average diet according to the population fraction of the two groups.

3.6.1. Caloric demand

Total annual caloric demand for plant-based food (*Cal_Dem*) is the sum of total plant-based caloric intake by the vegetarian population (*Pop_Veg*) and meat-eating population (*Pop_Meat*).

$$Cal\_Dem_{food}(t) = Intk\_Veg_{food}(t) \times Pop\_Veg(t) + Intk\_Meat_{food}(t) \times Pop\_Meat(t),$$
$$where\ food \in [pulses, grains, vegetables\ and\ fruits, other\ crops] \quad (19)$$

where $Intk\_Veg_{plant}$ and $Intk\_Meat_{plant}$ are the annual per-capita intake of plant-based calories in the vegetarian diet and meat-based diet, respectively. Both are assumed as a constant fraction of the annual total caloric intake per capita. Annual total caloric intake per capita is formulated as the multiplication of a reference intake per capita and the effect of income. The latter is a logistic function based on *GWP_per_Cap*.

Total annual caloric demand for animal-based food is simplified as

$$Cal\_Dem_{food}(t) = Intk\_Meat_{food}(t) \times Pop\_Meat(t),$$
$$where\ food \in [pasture - based\ meat, crop - based\ meat, dairy, eggs] \quad (20)$$

where $Intk\_Meat_{meat}$ is the annual per-capita intake of meat-based calories in the meat-based diet.

3.6.2. Food demand and food production

Food demand is calculated as Cal_Dem_{food} divided by the caloric value of associated food category. In addition, plant-based food categories are also be used as livestock feed. The amount of plant-based food used for feed depends on crop-based meat demand, feed share of four plant-based food, and unit-feed requirement for livestock. Food pro-

duction is eventually steered by waste-adjusted food demand, which is calculated as food demand divided by a waste fraction of supply. The waste fraction is set as 0.30 for grains, 45% for pulses, vegetables and fruits the waste fraction is 45%, and 20% for other food categories.

The production of animal-based food products (pasture-based meat, crop-based meat, dairy, and eggs) follows a similar approach based on grassland availability, food demand and land yield. Dairy production is aligned with meat production, and the production of eggs is formulated with respect to crop-based meat production, which depends on the feed fraction of crop production.

3.7. Carbon cycle

CO_2 emissions are calculated based on representations of carbon emissions from the energy and land-use change sectors. These emissions accumulate in the atmosphere until they are absorbed into the biosphere, pedosphere or oceans based on C-ROADS (Sterman et al., 2012, 2013).

3.7.1. Carbon emissions

Total carbon emission rates from the energy sector include carbon emission rates from fossil and renewable sources. Carbon emissions of a specified energy ($C\_Emis\_En_{energy}$) are based on the carbon intensity of energy production (C_Int_{energy}), which is calibrated to historical emissions within the uncertainty ranges of the unit emissions of energy
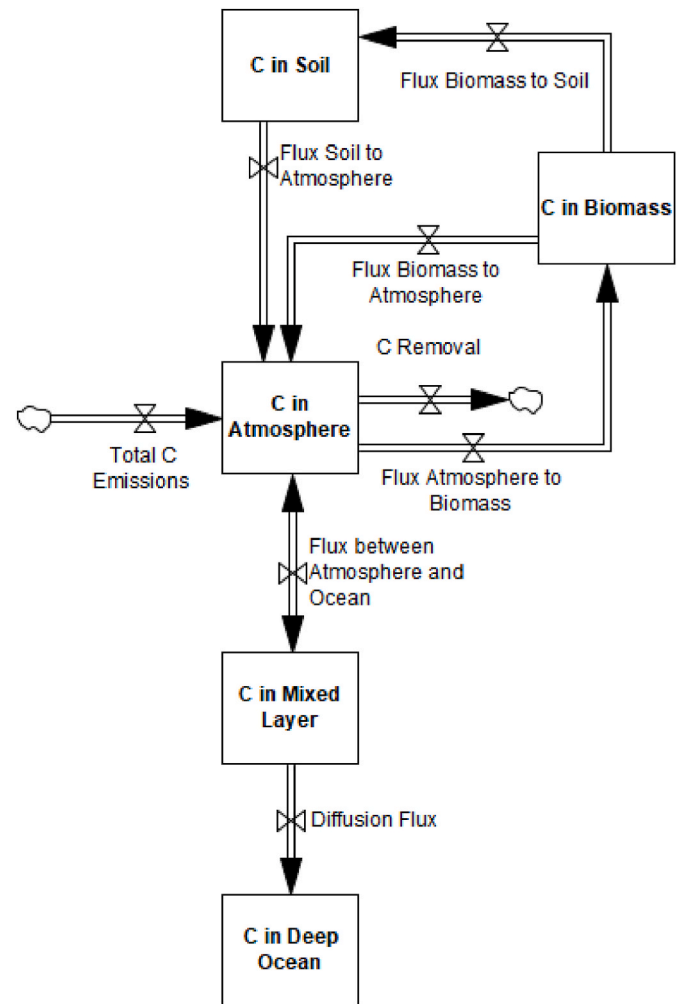

Fig. 7. Carbon stocks and associated flux among the stocks. Carbon accumulation in deep ocean is taken into account at four distinct ocean layers, yet not visualized for simplicity.

production (IPCC, 2014).

$$C\_Emis\_En_{energy}(t) = C\_Int_{energy} \times Prod_{energy}(t) \qquad (21)$$

where *Prod* represents the annual production of different types of energy. Carbon emissions of fossil fuels also include the effect of carbon capture and storage technology.

Carbon emissions from land-use change (*C_Emis_Land*) includes emissions from agricultural land change (*C_Emis_Agri*), and forest land change due to deforestation and forest conversion to managed forests and plantations (*C_Emis_Frst*).

$$C\_Emis\_Land(t) = C\_Int\_Agri \times Land\_Chg\_Agri(t) + C\_Int\_Frst$$
$$\times Land\_Chg\_Frst(t) \qquad (22)$$

where *C_Int_Agri* and *C_Int_Frst* represent carbon intensity of agricultural land use and forest land use, respectively. *Land_Chg_Agri* and *Land_Chg_Frst* represent ratio of agricultural and forest land area change compared to its initial area in year 1900.

3.7.2. Carbon stock

Stocks of carbon are considered in the atmosphere, biosphere, mixed ocean layer, and four deep ocean layers (Fig. 7). Carbon in the atmosphere (*C_Stk_Atm*) accumulates through total carbon emissions formulated above. Carbon in biosphere is captured in biomass (*C_Stk_Biom*) and soil (*C_Stk_Soil*). *C_Stk_Biom* includes carbon stock in leaves, branches, stems and roots, whereas *C_Stk_Soil* includes carbon stock in litter and humus. As the concentration of *C_Stk_Atm* rises, it forces increase of the uptake by ocean and biosphere. Carbon flux from the atmosphere to the biomass is modeled according to the formula in Wullschleger et al. (1995) and grows logarithmically as the concentration of *C_Stk_Atm* increases. The residence of *C_Stk_Biom* depends on average lifespan. The outflow of *C_Stk_Biom* is partitioned between carbon flux from the biomass to the atmosphere and to the humus according to humification fraction. The outflow from *C_Stk_Soil* is equal to its content divided by its average lifespan in the humus. The flux between *C_Stk_Atm* and carbon stock in the mixed ocean layer (*C_Stk_Ocn*) adjusts to an equilibrium that considers buffer factor, a measure of the resistance to atmospheric carbon dioxide being absorbed by the ocean surface layer. The buffer factor itself rises with the atmospheric concentration which decreases ocean absorption capacity. Deep ocean diffusion fluxes are modeled as a simple eddy-diffusion structure.

3.8. Climate

The climate module is based on the C-ROADS model (Sterman et al., 2012), which in turn refers to FREE model (Fiddaman, 2002) and DICE model (Nordhaus, 1992, 1994). The Earth's radiation budget is constrained to the temperature change due to carbon dioxide (CO_2), methane (CH_4), nitrous oxide (N_2O), halocarbons and other forcings (e. g., aerosols, O_3, etc.) CO_2 emissions are endogenous variables as described in the section **Carbon cycle**. The rest of forcings are generated exogenously based on historical data and the future projections from Representative Concentration Pathways (RCPs) (Byers et al., 2022). The temperature change is governed by radiative forcings, feedback cooling due to outbound longwave radiation, and heat transfer from the atmosphere and upper ocean to deep ocean layers.

3.8.1. Radiative forcing

Total radiative forcing consists of CO_2 radiative forcing due to increasing concentration of carbon in atmosphere, and other forcings which includes variables representing forcings from CH_4, N_2O, halocarbons and other gases and aerosols.

3.8.2. Feedback cooling

Feedback cooling due to outbound longwave radiation governs

feedback mechanism of the atmosphere and the upper ocean. The rate of cooling is determined by the climate sensitivity—a metric used to characterize the response of the global climate system to a given forcing. It is broadly defined as the equilibrium global mean surface temperature change following a doubling of atmospheric CO_2 concentration.

3.8.3. Heat transfer

The heat transfer into deeper layers of the ocean is modeled as a function of the eddy diffusion, which controls the movement of carbon through the deep ocean. Four different layers of deep ocean are considered.

3.9. Biodiversity

The biodiversity module is a simple structure representing population carrying capacity. The population is represented by global and encompassing all biomes mean species abundance (*MSA*). *MSA* is increased by species regeneration rate and decreased by species extinction rate. In addition, *MSA* approaching species carrying capacity (*Spec_Capa*) limits species regeneration and intensifies species extinction. This process is quantified as logistic functions and based on the ratio between *MSA* and *Spec_Capa*, and the regeneration factor and the extinction factor, respectively.

3.9.1. Species carrying capacity

Spec_Capa is calculated based on reference species carrying capacity (*Spec_Capa_Max*), representing maximum sustained population size, and influencing factors related to fertilizers consumption (*Imp_Fertz_on_Biodiv*), biomass production for energy purposes (*Imp_Biom_on_Biodiv*), climate damage (*Imp_CC_on_Biodiv*) and land use change (*Imp_Land_on_Biodiv*).

$$Spec\_Capa(t) = Spec\_Capa\_Max \times Imp\_Fertz\_on\_Biodiv(t)$$
$$\times Imp\_Biom\_on\_Biodiv(t) \times Imp\_CC\_on\_Biodiv(t) \times Imp\_Land\_on\_Biodiv(t)$$
$$(23)$$

The four influencing factors are estimated by logistic functions. In detail, *Imp_Fertz_on_Biodiv* is a logistic function of fertilizer consumption (including nitrogen, phosphate, and potash fertilizers). *Imp_Biom_on_Biodiv* consists of impacts from forest agriculture biomass production, which are logistic functions of related land areas. *Imp_CC_on_Biodiv* is adopted from climate impact on economy, as a logistic function of temperature change from preindustrial. *Imp_Land_on_Biodiv* takes into consideration changes of agricultural land, forest land, and other land compared to their initial areas.

4. Model outputs of FeliX 2.0

4.1. Calibration to the historic data

Simulation trajectories of key variables from different modules in FeliX 2.0 demonstrate a strong alignment with their respective historic data (Fig. 8). Fifteen key variables are selected from different modules based on the best availability of their historic data and their interdependencies with other variables in the whole FeliX 2.0. The model is calibrated for the period 1900–2022, mostly 1960–2022 depending on the data availability, and then projects to the future. The historic data for these variables are sourced from reputable repositories, including Wittgenstein Centre Human Capital Data Explorer (Wittgenstein Centre, 2020) for population, total fertility rate, education graduates; the World Bank Data (The World Bank, 2020) for GWP, GWP per capita, and global poverty rate; International Energy Agency (IEA, 2020) for energy demand; FAOSTAT (FAOSTAT, 2020b) for agricultural land, and total daily calorie supply per capita; IPCC (2014) for total C emission from energy sector; NASA GISS (2023) for temperature change from preindustrial; and European Environment Agency (EEA, 2020) for atmospheric concentrations of CO_2.
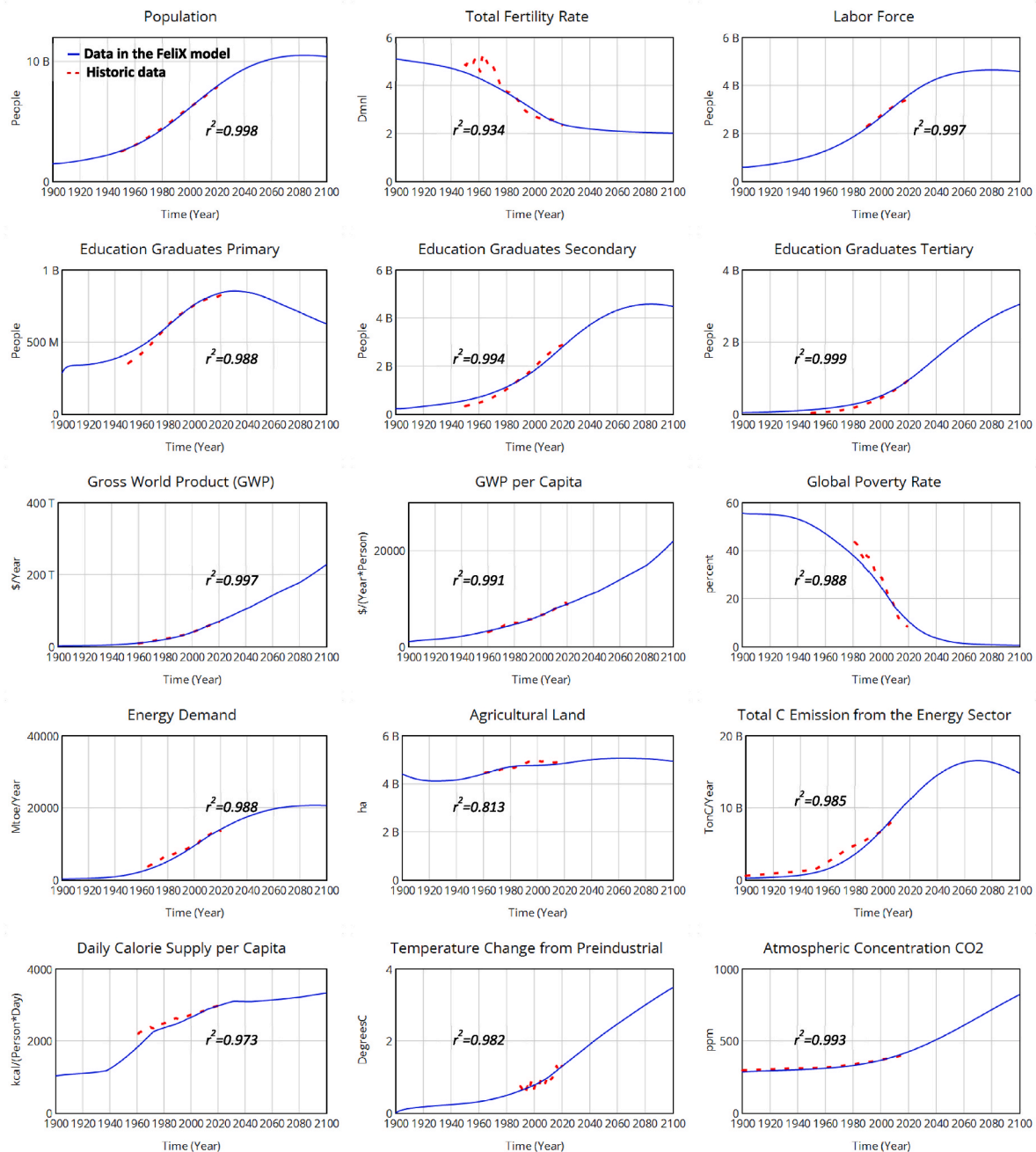
Fig. 8. Calibration results of key variables in FeliX 2.0. In the labels of ordinate, B stands for billions, Deg stands for degree, Dmnl stands for dimensionless, ha stands for hectare, Kcal stands for kilocalorie, Mtoe stands for million tonnes of oil equivalent, ppm stands for parts per million, T stands for trillions, and TonC stands for tonne of carbon.

The R square (R^2) values between trajectories simulated by FeliX 2.0 and historic data of these variables are more than 0.93 except of agricultural land ($R^2 = 0.81$) and temperature changes from preindustrial time ($R^2 = 0.84$). For the agricultural land, the low R^2 value can be attributed to the assumption that land use change, i.e. deforestation, is captured at higher aggregation level between forest and agricultural land, and a constant fraction of the total agricultural land is allocated to cropland and grassland. As for temperature changes from preindustrial time, the historic data per se were modeled such as observed with ±10% range of uncertainty according to (EEA, 2020; IPCC 2021). The best fitness is observed for the total population, total secondary graduates, total tertiary graduates, GWP, GWP per capita, and atmosphere CO_2 concentration. Their R^2 values are all more than 0.99. The best fitness of

these variables results from relatively more available data. As such, given the good reproduction of historical trends in FeliX 2.0, the model is able to capture the dynamic connections and interactions of the complex socio-economic and environmental system for simulating future development.

4.2. Future projections based on FeliX 2.0

The strong alignment of key variables with the historic data enables FeliX 2.0 to provide a more plausible future compared to existing IAM (Fig. 9). The projection outcomes of six variables in FeliX 2.0 are compared to those of key IAMs, namely the Global Change Assessment Model (GCAM), MESSAGE-GLOBIOM (Krey et al., 2020),
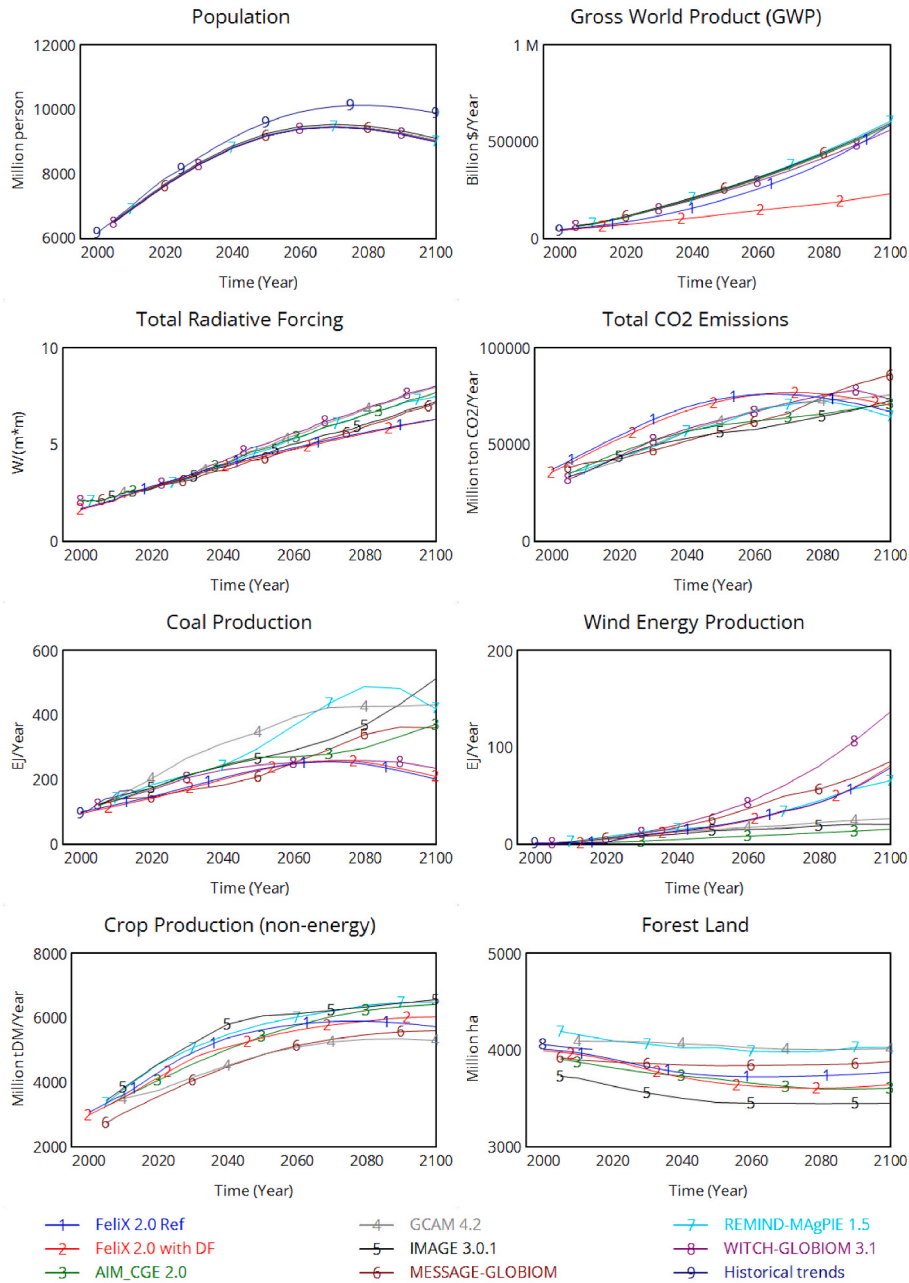
Fig. 9. Future projections of key variables under the shared socioeconomic pathway 2 (SSP2) in FeliX 2.0 and five existing IAMs. FeliX 2.0 Ref represents outputs from FeliX 2.0 without considering the climate impacts on economy, that is, the damage function (DF), while FeliX 2.0 with DF represents outputs from FeliX 2.0 with climate impacts. SSP2 projections by other models are obtained from the AR6 Scenario Database (Byers et al., 2022).

WITCH-GLOBIOM (Bosetti et al., 2006, 2009), AIM_CGE (Fujimori et al., 2017), IMAGE (Bouwman et al., 2006), and REMIND-MAgPIE (Luderer et al., 2013) using the IPCC AR6 Scenario Database (Byers et al., 2022). All projections follow the Shared Socioeconomic Pathway 2 (SSP2, O'Neill et al., 2017). Moreover, given that FeliX 2.0 particularly considers different damage functions in the economy module (see section **2.2.2. Climate change impacts on GWP**), projection results from FeliX 2.0 are further distinguished between FeliX 2.0 with and without damage functions (DFs).

The comparison shows that FeliX 2.0's projections fall within the ranges of results from selected IAMs, except for the total radiative forcing and GWP from FeliX 2.0 without DFs. Future total radiative forcing in both FeliX 2.0 is lower than those in other models. This can be attributed to our choice to use RCP4.5 projections for the non-CO_2 GHGs

in the baseline scenario of FeliX 2.0, in line with the current policies, while the SSP2 baseline corresponds approximately to RCP7.0. When considering DFs in economic outputs, future GWP would decrease by more than 50%. Whereas, if no DFs are considered in FeliX 2.0 either, future GWP would still be consistent with the SSP inputs to the other models (Dellink et al., 2017) which do not take climate impacts on economy into account. Total CO_2 emissions from the energy sector before 2080 in FeliX 2.0 are projected to be higher than those in other IAMs. The exclusion of carbon removal technologies such as carbon capture and storage under SSP2 is the main reason for the highest CO_2 emissions in FeliX 2.0. Coal production is relatively low while wind energy production is relatively high in FeliX 2.0 compared to the production in other selected models. It is because the market share of coal would shrink to 24% in 2100 while the share of coal in energy supply in

GCAM would be 30–50%. In addition, the market share of wind would expand to 12% in 2100 in FeliX 2.0. FeliX 2.0 results in relatively higher market shares of renewable energy (especially wind), resonating with the finding in Jaxa-Rozen and Trutnevyte (2021) about underestimation of the fast development of renewables by most IAMs. Projection results of crop production and forest land in FeliX 2.0s are both in line with results from other IAMs.

5. Limitations, outlooks, and conclusions

5.1. Limitations and outlooks

As a model developed for the purpose of capturing complex bio-physical and socioeconomic mechanisms at an aggregate level, FeliX 2.0 offers a comprehensive framework that addresses the limitations of conventional IAMs, notably the inattention to feedbacks and nonlinear interactions. The applications of FeliX 2.0 (see **Section 2**) in scenario analyses, emissions pathways, and sustainability assessments have proved its reliability as a useful tool for understanding global system dynamics and human well-being. However, FeliX 2.0 is also subject to several limitations. The first limitation arises from its global scale, preventing fine-scale analysis of socioeconomic-environmental dynamics. This hampers the effectiveness of FeliX 2.0 in devising targeted policies for localized challenges (e.g., water scarcity and deforestation) and hindering comprehensive solutions tailored to specific geographic contexts, given high heterogeneity across regions and nations. In addition, it also prevents FeliX 2.0 from adequately capturing the diverse contributions of specific regions, to specific global problems such as climate change. To address this limitation, it requires to add a regional dimension in associated modules in FeliX 2.0 such as population, economy, etc. In addition, each regionalized module should follow the global structure and be calibrated by historical data of each region, to make sure the consistency and robustness of generated results.

The second limitation is the relatively macro-modeling approach of different sectors in FeliX 2.0 that does not involve a high level of techno-economic detail. This reduces FeliX 2.0's ability to adequately capture the diverse contributions of specific sectors to specific global problems. For example, the end use sectors leading to the primary energy consumption are not modeled endogenously in FeliX 2.0. The transportation sector, for instance, accounted for around 30% and 20%, respectively, of global total energy consumption and CO_2 emissions in 2020 (IEA, 2022). Hence, it is also critical for climate mitigation through transitioning to electric vehicles, investing in public transportation, implementing sustainable traffic planning, and decarbonization in shipping and aviation (Jaramillo et al., 2022). To address the second limitation, more key sectors and factors of human-earth system can be added into FeliX 2.0 while focusing on the feedbacks rather than technoeconomic detail, as the distinguishing feature of FeliX. Lastly, FeliX 2.0 is a publicly available model, yet it requires a licensed software (Vensim DSS) for full functionality. A fully open access version of FeliX 2.0 can enhance its accessibility, transparency, open review, and collaboration, that are critical for robust and inclusive research.

5.2. Conclusions

The development and utilization of FeliX 2.0 have enabled understanding of global socioeconomic-environmental dynamics and their multilateral interactions. The robust calibration results of key variables within FeliX 2.0 modules against historic data highlights the model's efficacy in capturing the complex interdependencies of global systems since the beginning of the 20th century as they have been observed. Moreover, future projections from FeliX 2.0 exhibit coherence across multiple variables, including emissions, energy sector developments, crop production and forest land, compared to other existing IAMs. These insights highlight the strengths of FeliX 2.0 while also signaling avenues for refinement to enhance its usefulness and policy relevance, offering a

promising trajectory for robust long-term scenario simulations of global dynamics. The diverse applications of FeliX 2.0 in areas such as climate change, sustainable development, and global poverty elimination have provided evidence of its efficacy as a powerful tool for short- and long-term analyses of interested economic-environmental-social systems and existing global problems. However, FeliX 2.0 also have limitations that require future enhancements. Examples are its global scale and limited sector coverages. In summary, FeliX 2.0 stands as an informative tool for both SD and IAMs, and offers insights into the human-Earth system feedbacks. Overcoming its limitations will boost more potential of FeliX 2.0, enabling future research to design targeted policies and comprehensive solutions for a sustainable future.

Code and data availability

The FeliX model is publicly available at https://github.com/iiasa/Felix-Model. The model is developed in Vensim DSS, a licensed software, hence the full functionality of the model requires this software whereas it can be displayed freely by using Vensim Model Reader. Online model documentation can be seen at https://iiasa.github.io/felix_docs/.

CRediT authorship contribution statement

Quanliang Ye: Writing – original draft, Conceptualization. **Qi Liu:** Writing – original draft, Software, Methodology, Data curation. **Deepthi Swamy:** Writing – original draft, Software, Methodology. **Lei Gao:** Writing – original draft, Supervision. **Enayat A. Moallemi:** Writing – original draft, Supervision. **Felicjan Rydzak:** Writing – original draft, Supervision. **Sibel Eker:** Writing – original draft, Supervision, Software, Methodology, Funding acquisition, Conceptualization.

Declaration of competing interest

The authors declare that they have no known competing financial interests or personal relationships that could have appeared to influence the work reported in this paper.

Data availability

All the codes and data used in the model are stored in gitlab.com and fully open-accessed. This has been stated in the manuscript.

Acknowledgements

References

2030 Water Resources Group, 2009. Charting Our Water Future: Economic Frameworks to Inform Decision-Making.

Beck, M., Krueger, T., 2016. The epistemic, ethical, and political dimensions of uncertainty in integrated assessment modeling. WIREs Climate Change 7, 627–645. https://doi.org/10.1002/wcc.415.

Bosetti, V., Carraro, C., Galeotti, M., Massetti, E., Tavoni, M., 2006. WITCH A world induced technical change hybrid model. Energy J. 27, 13–37. http://www.jstor.org/stable/23297044.

Bosetti, V., Cian, E., Sgobbi, A., Tavoni, M., 2009. The 2008 WITCH Model: New Model Features and Baseline.

Bouwman, A.F., Kram, T., Klein Goldewijk, K., 2006. Integrated Modelling of Global Environmental Change - an Overview of IMAGE 2.4. Netherlands Environmental Assessment Agency (MNP), Bilthoven, The Netherlands.

Bressler, R.D., Moore, F.C., Rennert, K., Anthoff, D., 2021. Estimates of country level temperature-related mortality damage functions. Sci. Rep. 11, 20282 https://doi.org/10.1038/s41598-021-99156-5.

Burke, M., Hsiang, S.M., Miguel, E., 2015. Global non-linear effect of temperature on economic production. Nature 527, 235–239. https://doi.org/10.1038/nature15725.

Byers, E., Krey, V., Kriegler, E., Riahi, K., Schaeffer, R., Kikstra, J., Lamboll, R., Nicholls, Z., Sanstad, M., Smith, C., van der Wijst, K.-I., Khourdajie, A.A., Lecocq, F., Portugal-Pereira, J., Saheb, Y., Strømann, A., Winkler, H., Auer, C., Brutschin, E., Gidden, M., Hackstock, P., Harmsen, M., Huppmann, D., Kolp, P., Lepault, C.,

Lewis, J., Marangoni, G., Müller-Casseres, E., Skeie, R., Werning, M., Calvin, K., Forster, P., Guivarch, C., Hasegawa, T., Meinshausen, M., Peters, G., Rogelj, J., Samset, B., Steinberger, J., Tavoni, M., van Vuuren, D., 2022. AR6 Scenarios Database Hosted by IIASA. https://doi.org/10.5281/zenodo.5886911.

Calvin, K., Bond-Lamberty, B., 2018. Integrated human-earth system modeling—state of the science and future directions. Environ. Res. Lett. 13, 063006 https://doi.org/10.1088/1748-9326/aac642.

Davidsen, P.I., Sterman, J.D., Richardson, G.P., 1990. A petroleum life cycle model for the United States with endogenous technology, exploration, recovery, and demand. Syst. Dynam. Rev. 6, 66–93. https://doi.org/10.1002/sdr.4260060105.

Dellink, R., Chateau, J., Lanzi, E., Magné, B., 2017. Long-term economic growth projections in the shared socioeconomic pathways. Global Environ. Change 42, 200–214. https://doi.org/10.1016/j.gloenvcha.2015.06.004.

Dietz, S., Stern, N., 2015. Endogenous growth, convexity of damage and climate risk: how Nordhaus' framework supports deep cuts in carbon emissions. Econ. J. 125, 574–620. https://doi.org/10.1111/ecoj.12188.

Dixson-Declève, S., Gaffney, O., Ghosh, J., Randers, J., Rockström, J., Stoknes, P.E., 2022. Earth for All: a Survival Guide for Humanity: a Report to the Club of Rome (2022, Fifty Years after the Limits to Growth (1972). New Society Publishers, Gabriola Island, British Columbia, Canada.

Dumas, M., Frossard, E., Scholz, R.W., 2011. Modeling biogeochemical processes of phosphorus for global food supply. Chemosphere 84, 798–805. https://doi.org/10.1016/j.chemosphere.2011.02.039.

EEA, 2020. Trends in Atmospheric Concentrations of CO2 (Ppm), CH4 (Ppb) and N2O (Ppb), between 1800 and 2017.

Eker, S., Reese, G., Obersteiner, M., 2019. Modelling the drivers of a widespread shift to sustainable diets. Nat. Sustain. 2, 725–735. https://doi.org/10.1038/s41893-019-0331-1.

Eker, S., Liu, Q., Reiter, C., Kuhn, M., 2023. Full of Economic-Environment Linkages and Integration dX/dt (FeliX): Technical Model Documentation (No. ZVR 524808900). International Institute for Applied Systems Analysis (IIASA), Laxenburg, Austria.

Energy Institute, 2023. BP Statistical Review of World Energy, 2023.

FAO, 2018. Nutrient Phosphate P2O5 Fertilizers by Nutrient.

FAOSTAT, 2020a. Food Balance Sheets.

FAOSTAT, 2020b. Food and land-use data. http://www.fao.org/faostat/en/#home.

Fiddaman, T.S., 2002. Exploring policy options with a behavioral climate–economy model. Syst. Dynam. Rev. 18, 243–267. https://doi.org/10.1002/sdr.241.

Fosu, A.K., 2010. Inequality, income, and poverty: comparative global evidence. Soc. Sci. Q. 91, 1432–1446. https://doi.org/10.1111/j.1540-6237.2010.00739.x.

Fujimori, S., Hasegawa, T., Masui, T., 2017. AIM/CGE V2.0: basic feature of the model. In: Fujimori, S., Kainuma, M., Masui, T. (Eds.), Post-2020 Climate Action. Springer Singapore, Singapore, pp. 305–328. https://doi.org/10.1007/978-981-10-3869-3_13.

Hughes, B.B., 2015. International Futures (Ifs) Economic Model Documentation.

IEA, 2020. The international energy agency (IEA) data and statistics. https://www.iea.org/data-and-statistics/data-sets.

IEA, 2022. Energy Statistics Data Browser.

Intergovernmental Panel on Climate Change, 2021. Climate Change 2021 – the Physical Science Basis: Working Group I Contribution to the Sixth Assessment Report of the Intergovernmental Panel on Climate Change, first ed. Cambridge University Press. https://doi.org/10.1017/9781009157896.

Intergovernmental Panel On Climate Change (Ipcc), 2022a. In: Climate Change 2022 - Mitigation of Climate Change: Working Group III Contribution to the Sixth Assessment Report of the Intergovernmental Panel on Climate Change, first ed. Cambridge University Press. https://doi.org/10.1017/9781009157926.

Intergovernmental Panel On Climate Change (Ipcc), 2022b. Climate Change 2022 – Impacts, Adaptation and Vulnerability: Working Group II Contribution to the Sixth Assessment Report of the Intergovernmental Panel on Climate Change, first ed. Cambridge University Press. https://doi.org/10.1017/9781009325844.

IPCC, 2014. In: Climate Change 2014: Mitigation of Climate Change: Working Group III Contribution to the Fifth Assessment Report of the Intergovernmental Panel on Climate Change. Cambridge University Press, New York, NY.

Jaramillo, P., Kahn Ribeiro, S., Newman, P., Dhar, S., Diemuodeke, O.E., Kajino, T., Lee, D.S., Nugroho, S.B., Ou, X., Hammer Strømman, A., Whitehead, J., 2022. 2022: transport. In: Shukla, P.R., Skea, J., Slade, R., Al Khourdajie, A., van Diemen, R., McCollum, D., Pathak, M., Some, S., Vyas, P., Fradera, R., Belkacemi, M., Hasija, A., Lisboa, G., Luz, S., Malley, J. (Eds.), IPCC, 2022: Climate Change 2022: Mitigation of Climate Change. Contribution of Working Group III to the Sixth Assessment Report of the Intergovernmental Panel on Climate Change. Cambridge University Press, Cambridge, UK and New York, NY, USA.

Jaxa-Rozen, M., Trutnevyte, E., 2021. Sources of uncertainty in long-term global scenarios of solar photovoltaic technology. Nat. Clim. Change 11, 266–273. https://doi.org/10.1038/s41558-021-00998-8.

Kc, S., Wurzer, M., Speringer, M., Lutz, W., 2018. Future population and human capital in heterogeneous India. Proc. Natl. Acad. Sci. U.S.A. 115, 8328–8333. https://doi.org/10.1073/pnas.1722359115.

Krey, V., Havlik, P., Kishimoto, P., Fricko, O., Zilliacus, J., Gidden, M., Strubegger, M., Kartasasmita, G., Ermolieva, T., Forsell, N., Guo, F., Gusti, M., Huppmann, D., Johnson, N., Kikstra, J., Kindermann, G., Kolp, P., Lovat, F., McCollum, D., Min, J., Pachauri, S., Parkinson, S., Rao, S., Rogelj, J., Ünlü, G., Valin, H., Wagner, P., Zakeri, B., Obersteiner, M., Riahi, K., 2020. MESSAGEix-GLOBIOM Documentation - 2020 release. https://doi.org/10.22022/IACC/03-2021.17115.

Kuhn, M., Eker, S., Liu, Q., 2023. Global Systems Analysis for Understanding the Drivers of Sustainable Wellbeing, Systems Analysis for Sustainable Wellbeing—50 Years of IIASA Research, 40 Years after the Brundtland Commission, Contributing to the Post-2030 Global Agenda. International Institute for Applied Systems Analysis (IIASA), Laxenburg, Austria.

Lakner, C., Mahler, D.G., Negre, M., Prydz, E.B., 2022. How much does reducing inequality matter for global poverty? J. Econ. Inequal. 20, 559–585. https://doi.org/10.1007/s10888-021-09510-w.

Liu, Q., Gao, L., Guo, Z., Dong, Y., Moallemi, E.A., Eker, S., Yang, J., Obersteiner, M., Bryan, B.A., 2023a. Robust strategies to end global poverty and reduce environmental pressures. One Earth 6, 392–408. https://doi.org/10.1016/j.oneear.2023.03.007.

Liu, Q., Yang, J., Gao, L., Dong, Y., Guo, Z., Moallemi, E.A., Eker, S., Obersteiner, M., 2023b. Robust sensitivity analysis to uncertainties in environmental and socio-economic scenarios: a perspective from a global socio-ecological system model. J. Clean. Prod. 410, 137244 https://doi.org/10.1016/j.jclepro.2023.137244.

Lontzek, T.S., Cai, Y., Judd, K.L., Lenton, T.M., 2015. Stochastic integrated assessment of climate tipping points indicates the need for strict climate policy. Nat. Clim. Change 5, 441–444. https://doi.org/10.1038/nclimate2570.

Lopez, A.D., Murray, C.C.J.L., 1998. The global burden of disease, 1990–2020. Nat. Med. 4, 1241–1243. https://doi.org/10.1038/3218.

Luderer, G., Leimbach, M., Bauer, N., Kriegler, E., Aboumahboub, T., Curras, T.A., Baumstark, L., Bertram, C., Giannousakis, A., Hilaire, J., Klein, D., Mouratiadou, I., Pietzcker, R., Piontek, F., Roming, N., Schultes, A., Schwanitz, V.J., Strefler, J., 2013. Description of the REMIND model (version 1.5). SSRN Journal. https://doi.org/10.2139/ssrn.2312844.

MacDonald, G.K., Bennett, E.M., Potter, P.A., Ramankutty, N., 2011. Agronomic phosphorus imbalances across the world's croplands. Proc. Natl. Acad. Sci. U.S.A. 108, 3086–3091. https://doi.org/10.1073/pnas.1010808108.

Meadows, D.H., Wright, D., 2008. Thinking in Systems: a Primer. Chelsea Green Pub, White River Junction, Vt.

Meadows, D.H., Meadows, D.L., Randers, J., Behrens, I.I.I.W.W. (Eds.), 1972. The Limits to Growth: a Report for the Club of Rome's Project on the Predicament of Mankind. Universe Books, New York.

Millennium Institute, 2021. iSDG: Documentation.

Moallemi, E.A., Bertone, E., Eker, S., Gao, L., Szetey, K., Taylor, N., Bryan, B.A., 2021. A review of systems modelling for local sustainability. Environ. Res. Lett. 16, 113004 https://doi.org/10.1088/1748-9326/ac2f62.

Moallemi, E.A., Eker, S., Gao, L., Hadjikakou, M., Liu, Q., Kwakkel, J., Reed, P.M., Obersteiner, M., Guo, Z., Bryan, B.A., 2022a. Early systems change necessary for catalyzing long-term sustainability in a post-2030 agenda. One Earth 5, 792–811. https://doi.org/10.1016/j.oneear.2022.06.003.

Moallemi, E.A., Gao, L., Eker, S., Bryan, B.A., 2022b. Diversifying models for analysing global change scenarios and sustainability pathways. Glob. Sustain. 5, e7. https://doi.org/10.1017/sus.2022.7.

NASA GISS, 2023. GISS Surface Temperature Analysis (GISTEMP), version 4.

Nordhaus, W.D., 1992. The "dice" model: background and structure of a dynamic integrated climate-economy model of the economics of global warming. Cowles Foundation Discussion Papers, 1252.

Nordhaus, W.D., 1993. Optimal greenhouse-gas reductions and tax policy in the "DICE" model. Am. Econ. Rev. 83, 313–317.

Nordhaus, W.D., 1994. Managing the global commons. The Economics of Climate Change. MIT Press, MA.

Nordhaus, W.D., 2017. Revisiting the social cost of carbon. Proc. Natl. Acad. Sci. U.S.A. 114, 1518–1523. https://doi.org/10.1073/pnas.1609244114.

Obersteiner, M., Rydzak, F., Fritz, S., McCallum, I., 2012. Valuing the potential impacts of GEOSS: a systems dynamics approach. In: Laxminarayan, R., Macauley, M.K. (Eds.), The Value of Information. Springer, Netherlands, Dordrecht, pp. 67–90. https://doi.org/10.1007/978-94-007-4839-2_4.

O'Neill, B.C., Kriegler, E., Ebi, K.L., Kemp-Benedict, E., Riahi, K., Rothman, D.S., Van Ruijven, B.J., Van Vuuren, D.P., Birkmann, J., Kok, K., Levy, M., Solecki, W., 2017. The roads ahead: narratives for shared socioeconomic pathways describing world futures in the 21st century. Global Environ. Change 42, 169–180. https://doi.org/10.1016/j.gloenvcha.2015.01.004.

Pedercini, M., Arquitt, S., Chan, D., 2020. Integrated simulation for the 2030 agenda. Syst. Dynam. Rev. 36, 333–357. https://doi.org/10.1002/sdr.1665.

Pimentel, D., Pimentel, M., 2003. Sustainability of meat-based and plant-based diets and the environment. Am. J. Clin. Nutr. 78, 660S–663S. https://doi.org/10.1093/ajcn/78.3.660S.

Pye, S., Sabio, N., Strachan, N., 2015. An integrated systematic analysis of uncertainties in UK energy transition pathways. Energy Pol. 87, 673–684. https://doi.org/10.1016/j.enpol.2014.12.031.

Ranganathan, J., Vennard, D., Waite, R., Lipinski, B., Searchinger, T., Dumas, P., 2016. Shifting diets for a sustainable food future: creating a sustainable food future. Working Paper, Installment 11 of Creating a Sustainable Food Future. World Resources Institute, Washington, DC. Accessible at. http://www.worldresourcesreport.org.

Riahi, K., Van Vuuren, D.P., Kriegler, E., Edmonds, J., O'Neill, B.C., Fujimori, S., Bauer, N., Calvin, K., Dellink, R., Fricko, O., Lutz, W., Popp, A., Cuaresma, J.C., Kc, S., Leimbach, M., Jiang, L., Kram, T., Rao, S., Emmerling, J., Ebi, K., Hasegawa, T., Havlik, P., Humpenöder, F., Da Silva, L.A., Smith, S., Stehfest, E., Bosetti, V., Eom, J., Gernaat, D., Masui, T., Rogelj, J., Strefler, J., Drouet, L., Krey, V., Luderer, G., Harmsen, M., Takahashi, K., Baumstark, L., Doelman, J.C., Kainuma, M., Klimont, Z., Marangoni, G., Lotze-Campen, H., Obersteiner, M., Tabeau, A., Tavoni, M., 2017. The Shared Socioeconomic Pathways and their energy, land use, and greenhouse gas emissions implications: an overview. Global Environ. Change 42, 153–168. https://doi.org/10.1016/j.gloenvcha.2016.05.009.

Ruan, W., Guo, Z., Yang, J., Gao, L., Dong, Y., Liu, Q., 2023. Assessing the progress toward achieving energy- and climate-related sustainable development goals under

four global energy transition outlooks. Sustain. Dev. 2873 https://doi.org/10.1002/sd.2873 sd.

Rydzak, F., Obersteiner, M., Kraxner, F., Fritz, S., McCallum, I., 2013. FeliX3–Impact Assessment Model: Systemic View across Societal Benefit Areas beyond Global Earth Observation. International Institute for Applied Systems Analysis (IIASA). Laxenburg.

Schneider, S.H., 1997. Integrated assessment modeling of global climate change: transparent rational tool for policy making or opaque screen hiding value-laden assumptions? Environ. Model. Assess. 2, 229–249. https://doi.org/10.1023/A:1019090117643.

Schwanitz, V.J., 2013. Evaluating integrated assessment models of global climate change. Environ. Model. Software 50, 120–131. https://doi.org/10.1016/j.envsoft.2013.09.005.

Sterman, J., 2000. Business Dynamics: Systems Thinking and Modeling for a Complex World. Irwin/McGraw-Hill, Boston.

Sterman, J.D., Richardson, G.P., 1985. An experiment to evaluate methods for estimating fossil fuel resources. J. Forecast. 4, 197–226. https://doi.org/10.1002/for.3980040208.

Sterman, J., Fiddaman, T., Franck, T., Jones, A., McCauley, S., Rice, P., Sawin, E., Siegel, L., 2012. Climate interactive: the C-ROADS climate policy model. Syst. Dynam. Rev. 28, 295–305. https://doi.org/10.1002/sdr.1474.

Sterman, J.D., Fiddaman, T., Franck, T., Jones, A., McCauley, S., Rice, P., Sawin, E., Siegel, L., 2013. Management flight simulators to support climate negotiations. Environ. Model. Software 44, 122–135. https://doi.org/10.1016/j.envsoft.2012.06.004.

The World Bank, 2020. World Bank Open Data.

The World Bank, 2022. Fact Sheet: an Adjustment to Global Poverty Lines.

USDA, 2020. USDA Food Composition Databases.

Van Beek, L., Hajer, M., Pelzer, P., Van Vuuren, D., Cassen, C., 2020. Anticipating futures through models: the rise of Integrated Assessment Modelling in the climate science-policy interface since 1970. Global Environ. Change 65, 102191. https://doi.org/10.1016/j.gloenvcha.2020.102191.

Van Vuuren, D.P., Batlle Bayer, L., Chuwah, C., Ganzeveld, L., Hazeleger, W., Van Den Hurk, B., Van Noije, T., O'Neill, B., Strengers, B.J., 2012. A comprehensive view on climate change: coupling of earth system and integrated assessment models. Environ. Res. Lett. 7, 024012 https://doi.org/10.1088/1748-9326/7/2/024012.

Van Vuuren, D.P., Van Soest, H., Riahi, K., Clarke, L., Krey, V., Kriegler, E., Rogelj, J., Schaeffer, M., Tavoni, M., 2016. Carbon budgets and energy transition pathways. Environ. Res. Lett. 11, 075002 https://doi.org/10.1088/1748-9326/11/7/075002.

Walsh, B.J., Rydzak, F., Palazzo, A., Kraxner, F., Herrero, M., Schenk, P.M., Ciais, P., Janssens, I.A., Peñuelas, J., Niederl-Schmidinger, A., Obersteiner, M., 2015. New feed sources key to ambitious climate targets. Carbon Bal. Manag. 10, 26. https://doi.org/10.1186/s13021-015-0040-7.

Walsh, B., Ciais, P., Janssens, I.A., Peñuelas, J., Riahi, K., Rydzak, F., Van Vuuren, D.P., Obersteiner, M., 2017. Pathways for balancing CO2 emissions and sinks. Nat. Commun. 8, 14856 https://doi.org/10.1038/ncomms14856.

Wittgenstein Centre, 2020. Wittgenstein Centre Human Capital Data Explorer. http://dataexplorer.wittgensteincentre.org/wcde-v2/.

Wullschleger, S.D., Post, W.M., King, A.W., 1995. On the potential for a CO2 fertilization effect in forests: estimates of the biotic growth factor based on 58 controlled-exposure studies. In: Woodwell, G.M., Mackenzie, F.T. (Eds.), Biotic Feedbacks in the Global Climatic System. Oxford University PressNew, York, NY, pp. 85–107. https://doi.org/10.1093/oso/9780195086409.003.0005.

Yang, J., Gao, L., Liu, Q., Guo, Z., 2023. Assessing environmental impacts of response strategies for sustainable food system transformation. Sustainable Development sd 2795. https://doi.org/10.1002/sd.2795.

Ye, Q., Eker, S., 2024. The FeliX 2.0 webpage: overview of the underlying modeling methodology and links to the FeliX 2.0 resources and publications. https://iiasa.github.io/felix_docs/.

Yin, X., Struik, P.C., 2010. Modelling the crop: from system dynamics to systems biology. J. Exp. Bot. 61, 2171–2183. https://doi.org/10.1093/jxb/erp375.